frontiers in Cellular Neuroscience

METHODS
published: 13 January 2016
doi: 10.3389/fncel.2015.00514

A Novel Method for the Description of Voltage-Gated Ionic Currents Based on Action Potential Clamp Results—Application to Hippocampal Mossy Fiber Boutons

John R. Clay *

Department of Physiology, National Institute of Neurological Disorders and Stroke, National Institutes of Health, Rockville, MD, USA

Action potential clamp (AP-clamp) recordings of the delayed rectifier K^+ current I_K and the fast-activated Na^+ current I_{Na} in rat hippocampal mossy fiber boutons (MFBs) are analyzed using a computational technique recently reported. The method is implemented using a digitized AP from an MFB and computationally applying that data set to published models of I_K and I_{Na}. These numerical results are compared with experimental AP-clamp recordings. The I_{Na} result is consistent with experiment; the I_K result is not. The difficulty with the I_K model concerns the fully activated current-voltage relation, which is described here by the Goldman-Hodgkin-Katz dependence on the driving force (V-E_K) rather than (V-E_K) itself, the standard model for this aspect of ion permeation. That revision leads to the second—a much steeper voltage dependent activation curve for I_K than the one obtained from normalization of a family of I_K records by (V-E_K). The revised model provides an improved description of the AP-clamp measurement of I_K in MFBs compared with the standard approach. The method described here is general. It can be used to test models of ionic currents in any excitable cell. In this way it provides a novel approach to the relationship between ionic current and membrane excitability in neurons.

Keywords: rat hippocampus, action potential clamp, mathematical models, Goldman-Hodgkin-Katz, ion channels

OPEN ACCESS

Edited by:
Lavinia Alberi,
University of Fribourg, Switzerland

Reviewed by:
Euan Robert Brown,
Heriot Watt University, UK
Ping Liu,
University of Connecticut Health Center, USA

***Correspondence:**
John R. Clay
jrclay@ninds.nih.gov

Received: *23 September 2015*
Accepted: *21 December 2015*
Published: *13 January 2016*

Citation:
Clay JR (2016) A Novel Method for the Description of Voltage-Gated Ionic Currents Based on Action Potential Clamp Results—Application to Hippocampal Mossy Fiber Boutons. Front. Cell. Neurosci. 9:514. doi: 10.3389/fncel.2015.00514

INTRODUCTION

The action potential clamp technique (AP-clamp) is a paradigm in which an AP recorded from a neuron in current clamp is applied to that same cell in voltage clamp mode before and after the addition of a specific ion channel blocker to the external medium (Llinás et al., 1982; Bean, 2007). In this way the role of that current during an AP can be determined. The AP can also be applied computationally to a mathematical model of that current constructed from voltage step results in order to provide an additional test of the model. This approach was recently applied to $I_{Na}$and I_{Ca} in suprachiasmatic nucleus neurons (Jackson et al., 2004; Clay, 2015). In this report the method is applied to the AP-clamp recordings of Alle et al. (2009) of I_{Na} and I_K in rat hippocampal mossy fiber boutons (MFBs) at physiological temperatures ($T = 36 - 37^{\circ}$C). Those results demonstrate a significant separation in time during an AP of I_{Na} and I_K, an important result for efficient neuronal signaling (Crotty et al., 2006; Alle et al., 2009; Sengupta et al., 2010). The method was

implemented using digitized results from MFBs (personal communication, Dr. H. Alle). A digitized representation of an AP from an MFB was applied computationally to the models of I_K and I_{Na} in MFBs of Engel and Jonas (2005) for model testing. The I_K AP-clamp analysis revealed a significant discrepancy between theory and experiment, which can be resolved using the Goldman-Hodgkin-Katz (GHK) equation for the fully activated current-voltage relation for I_K (Clay, 2009). The revised I_K model provides a significant improvement in the description of this component compared with a model in which a linear dependence of I_K on (V-E_K) was used. Computational analysis of the I_{Na} AP-clamp result (Alle et al., 2009) using the Engel and Jonas (2005) I_{Na} model was in agreement with experiment.

MATERIALS AND METHODS

A data set corresponding to an AP from MFBs was applied computationally to the models of I_K and I_{Na} of Engel and Jonas (2005) which are given by $I_K = g_K n^4(V\text{-}E_K)$ and $I_{Na} = g_{Na} m^3 h(V\text{-}E_{Na})$, respectively, similar to the original models of I_K and I_{Na} in squid giant axons of Hodgkin and Huxley (1952), with g_K and g_{Na}constants, E_K and E_{Na} the K^+, and Na^+ reversal potentials and

$$dx/dt = -(\alpha_x + \beta_x)x + \alpha_x \quad (1)$$

with x = n, m, or h, and time t in msec. The rate parameters in Equation (1) are given by Engel and Jonas (2005).

$$\begin{aligned} \alpha_n &= -0.01(V+55)/\{\exp[-(V+55)/10]-1\}; \\ \beta_n &= 0.125\exp[-(V+65)/80] \quad (2) \\ \alpha_m &= -93.8(V-105)/\{\exp[-(V-105)/17.7)-1\}; \\ \beta_m &= 0.17\exp(-V/23.3) \\ \alpha_h &= 0.00035\exp(-V/18.7); \\ \beta_h &= 6.6/\{\exp[-(V+17.7)/13.3]+1\}. \quad (3) \end{aligned}$$

The expressions for α_n and β_n (Equation 2) were taken from the experimental procedures of Engel and Jonas (2005). The expressions for α_m, β_m, α_h, and β_h (Equation 3) were taken from Supplementary Table 1 of their paper. All αs and βs in Equations (2) and (3) are in units of inverse milliseconds. The model of I_K was based on the voltage step recordings of this component in MFBs by Geiger and Jonas (2000) obtained at $T = 34°C$. It was extrapolated to $T = 37°C$ using a Q_{10} of 2.2 (Fohlmeister, 2015). That is, α_n and β_n (Equation 2) were each multiplied by 1.27. The reversal potential for K^+ used in the analysis was $E_K = -110$ mV. [$E_K = kT/q \ln(K_o^+/K_i^+)$ where k is the Boltzmann constant, T is the absolute temperature, q is the unit electron charge (kT/q = 26.7 mV for $T = 37°C$), K_o^+=2.5 mM and K_i^+ = 155 mM (Alle et al., 2009)]. The recordings of I_{Na} of Engel and Jonas (2005) were obtained at $T = 23°C$. Their model of I_{Na} was extrapolated to $T = 37°$by multiplying each of the αs and βs in Equation (3) by a factor of 2.8. The reversal potential for Na^+ was $E_{Na} = 62$ mV (Alle et al., 2009).

The V_i vs. t_i data set (i = 1,2,3. . . ; Supplementary Table 1) of the MFB AP from Figure 1B of Alle et al. (2009) is represented in the top panel of **Figure 1** with lines connecting adjacent points. It was applied to Equation (1) with $x = n$, m, or h using NDSolve in Mathematica (Wolfram Research, Inc., Champaign, IL). At $t_1 = 0$, $V_1 = -80$ mV. The initial value of n, n_1, was given by $\alpha_n/(\alpha_n+\beta_n)$ with $V = -80$ mV and $\alpha_n$and β_n given by Equation (2), i.e., $n_1 = 0.1288$. The following point of the AP data set is $t_2 = 0.039$ ms, $V_2 = -77.7$ mV. The corresponding value of n,n_2, was determined from Equation (1) and NDSolve using $V(t) = V_1+(V_2-V_1)(t-t_1)/(t_2-t_1)$ for $t_1 < t < t_2$. The result was $n_2 = 0.1289$. More significant changes in n occur later as the membrane potential is depolarized throughout the AP. A similar analysis was applied to $x = m$ and h.

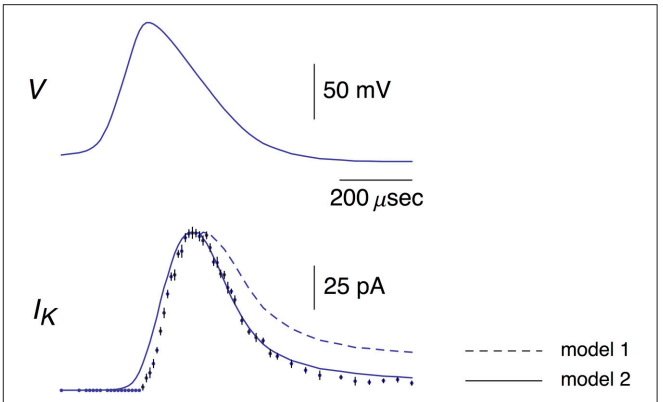

FIGURE 1 | Top panel: This AP corresponds to the AP in the top panel of Figure 1B from Alle et al. (2009). A digitized version of this waveform is given in Supplementary Table 1. The points in that data set were connected by lines to given the result shown. **Bottom panel**: The data points with error bars (n = 9; ±SEM) correspond to AP-clamp measurements of I_K in MFBs (Alle et al., 2009). The mean values of these results are also given in Supplementary Table 1. The theoretical results (models 1 and 2) are as described in the text.

RESULTS

K^+ Current

A digital representation of the AP-clamp recordings of I_K from Alle et al. (2009) is given in the bottom panel of **Figure 1** of this report (data points with the error bars representing ±SEM, n = 9; Supplementary Table 1). These results are the differences obtained by application of the AP in **Figure 1** to MFBs in voltage-clamp before and after addition to the bath of 1 mM 4-aminopyridine (4-AP), which was sufficient to completely block I_K elicited by an AP (Alle et al., 2009, 2011). They were scaled to match the I_K result in the bottom panel of Figure 1B of Alle et al. (2009). Also shown in **Figure 1** is the prediction of the Engel and Jonas (2005) I_K model (dashed line; model 1) starting from the maximum level of I_K close to the peak of the AP. The rising phase of the model is not shown. These results (also given in Supplementary Table 1) correspond to $I_{K,i} = g_K n_i^4(V_i\text{-}E_K)$, i = 1.2.3. . . , with n_i determined as described above (Section Materials and Methods), $E_K = -110$ mV, and $g_K = 36$ mS/cm^2. This model—model 1, the Engel and Jonas (2005) I_K model—does not provide a good description of the I_K AP-clamp result. The difficulty most likely concerns the fully

activated current-voltage relation for I_K. This result for squid axons is well described by the GHK dependence on (V-E_K) rather than by (V-E_K) itself (Clay et al., 2008), a relationship given by $I_K(n = 1) = a\text{GHK}[(V\text{-}E_K)]$ where a is a constant, and GHK[(V-E_K)] = (qV/kT) {exp[q(V-E_K)/kT]-1}/[exp(qV/kT)-1]. In their original analysis of squid axon currents Hodgkin and Huxley (1952) obtained the I_K activation curve, an important result for models of I_K, by normalizing a family of I_K records with (V-E_K), a linear dependence on driving force. Normalization by GHK[(V-E_K)] should be used instead. This analysis is illustrated for I_K from MFBs in **Figure 2** using the results of Geiger and Jonas (2000). Their $I_K$activation curve is shown in **Figure 2** (open circles) along with a description of this result by $n_\infty^4(V)$ with $n_\infty(V) = \alpha_n/(\alpha_n + \beta_n)$ and α_n and β_n as given above (Equation 2). Their result for $V = 50$ mV (Figure 1C of Geiger and Jonas, 2000) was not included. The I_K component in squid axons is partially blocked by Na_i^+ in a voltage-dependent manner for strong depolarizations such as $V \geq 50$ mV (Bezanilla and Armstrong, 1972; French and Wells, 1977). Geiger and Jonas (2000) used an intracellular solution containing 21 mM Na^+. A partial block of I_K in MFBs at 50 mV by this level of Na_i^+ cannot be ruled out and so this point was excluded from the analysis. The remaining results from $V = -70$ to $+30$ mV were multiplied by (V-E_K) to remove the linear normalization they used to obtain their result. The next step was normalization with GHK[(V-E_K)] as described in Clay (2009)—closed circles in **Figure 2**. The result is an I_K activation curve that is significantly steeper than the one obtained using normalization by (V-E_K). A single modification in the Engel and Jonas (2005) model is sufficient to describe these results, namely a change in β_n from 0.125 exp[$-$(V+65)/80] ms^{-1} to 0.125 exp[$-$(V+65)/20] ms^{-1}, the curve labeled "n_∞^4 revised" in **Figure 2**. The same modification in the original Hodgkin and Huxley (1952) model, namely replacing "80" in the exponential term of β_n to "20," is sufficient to describe the I_K activation curve in squid axons obtained using GHK normalization of a family of I_K records (Clay et al., 2008). The AP-clamp result for this version of the Engel and Jonas (2005) I_K model—model 2—is given by an_i^4 GHK[(V_i-E_K)], continuous line in **Figure 1**, with $a = 1.3$ mA/cm^2 and n_i determined from Equation (1) using the modified version of β_n. This result provides a significant improvement in the description of the falling phase of the experimental record compared with model 1. The rising phase of both models underestimates the delay in the rise of I_K during an AP, a result that is similar to the Cole and Moore (1960) effect for voltage steps in squid axons (Discussion).

The revised I_K result in **Figure 1**—model 2—is further illustrated by the current-voltage trajectory for I_K during the AP in **Figure 1** (**Figure 3**—dashed line). The I_K gate—the n variable—is maximally activated during the AP to a level of 0.283, which occurs near the latter part of the repolarization phase. The GHK current voltage relation with $n = 0.283$, also shown in **Figure 3**, is tangent to the trajectory at this point (arrow labeled **a**). The trajectory lies close to the GHK relation a considerable distance on either side of **a**, indicating that the time course of I_K in model 2 during repolarization is largely determined by the GHK equation.

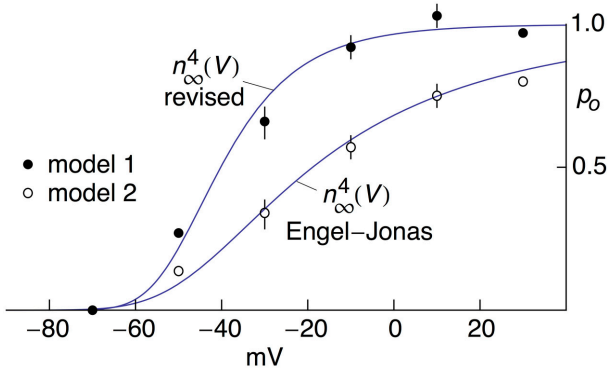

FIGURE 2 | Open channel probability, p_o, for I_K in MFB's as a function of V. The open circles were taken from Figure 5C from Geiger and Jonas (2000). The curve describing those results corresponds to $n_\infty^4(V)$ with $n_\infty(V) = \alpha_n/(\alpha_n + \beta_n)$ and $\alpha_n = -0.01(V+55)/\{\exp[-(V+55)/10]-1\}$ msec^{-1}, $\beta_n = 0.125\ \exp[-(V+65)/80]$ msec^{-1} (Engel and Jonas, 2005). These results were obtained from normalization of a family of I_K records with (V-E_K) and $E_K = -85$ mV (Geiger and Jonas, 2000). They were multiplied by (V+85) and renormalized using GHK[($V-E_K$)] as described in the text with kT/q=26.5 mV ($T = 34°$C) and $E_K = -104$ mV from $K_o = 2.5$ mM and $K_i = 125$ mM (Geiger and Jonas, 2000). The renormalized results are represented by the filled circles. The theoretical curve describing those results is given by $n_\infty^4(V)$ with $\alpha_n = -0.01(V+55)/\{\exp[-(V+55)/10]-1\}$ msec^{-1} and $\beta_n = 0.125\ \exp[-(V+65)/20]$ msec^{-1}.

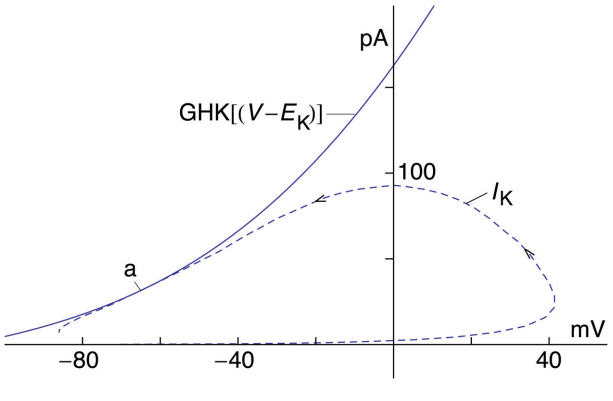

FIGURE 3 | Current-voltage trajectory (dashed line) of I_K—model 2—for the AP in Figure 1. The arrows indicate the direction of time. Also shown is the GHK current-voltage relation, an^4 GHK(V-E_K) with $a = 1.3$ mA/cm^2, $n = 0.283$, and GHK(V-E_K) as given in the text. The I_K trajectory during the AP is tangent to the GHK relation at point **a**.

Na^+ Current

Activation curve results for I_{Na} from MFBs—both experimental and theoretical—taken from Engel and Jonas (2005) are shown in **Figure 4** along with the revised I_K results described above. The I_K and I_{Na} activation curves overlap almost completely (**Figure 4**) an observation that may be consistent with known structural similarities of voltage-gated Na^+ and K^+ channels (MacKinnon, 1991, 1995; Jan and Jan, 1997; Hanlon and Wallace, 2002).

Pooled results of AP-clamp recordings of I_{Na} from Alle et al. (2009) are illustrated in **Figure 5** (data points with error bars

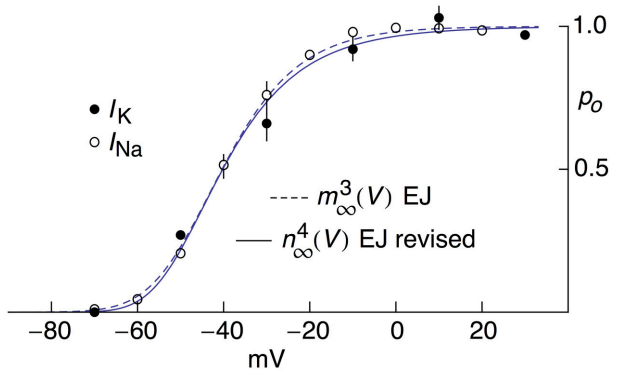

FIGURE 4 | Open channel probability, p_o, for I_K and I_{Na} for MFBs as a function of V, both experimental and theoretical. The experimental results for I_K were taken from Figure 5C of Geiger and Jonas (2000) as modified in **Figure 2**. The solid line labeled "$n^{4\infty}(V)$ EJ revised" corresponds to $[\alpha_n/(\alpha_n+\beta_n)]^4$ with $\alpha_n = -0.01(V+55)/\{\exp[-(V+55)/10]-1\}$ msec^{-1} and $\beta_n = 0.125\ \exp[-(V+65)/20]$ msec^{-1}. The experimental results for I_{Na} were taken from Figure 2B of Engel and Jonas (2005). The dashed curve labeled "$m^{3\infty}(V)$ EJ" corresponds to $[\alpha_m/(\alpha_m+\beta_m)]^3$ with $\alpha_m = -93.8(V-105)/\{\exp[-(V-105)/17.7]-1\}$ msec^{-1} and $\beta_m = 0.17\ \exp(-V/23.3)$ msec^{-1}.

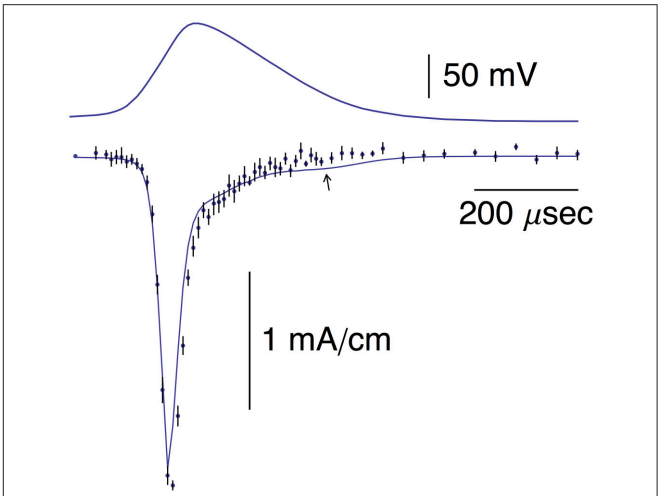

FIGURE 5 | Top panel: Same AP as in the top panel of **Figure 1**. **Bottom panel:** The data points with error bars ($n = 8$; ±SEM) correspond to AP-clamp measurements of I_{Na} in MFBs (Alle et al., 2009). The mean values of those results are also given in Supplementary Table 1. The theoretical curve is as described in the text.

representing ±SEM, $n = 9$; Supplementary Table 1). They were scaled to match the I_{Na} result in the bottom panel of Figure 2B of Alle et al. (2009). The results are the differences obtained by applying the AP shown in the top panel of **Figure 5** to MFBs before and after the addition of 1 μM tetrodotoxin (TTX) to the bathing medium. Also shown in **Figure 5** is the prediction of the Engel and Jonas (2005) model described above, $I_{Na,i} = g_{Na} m_i^3 h_i (V_i\text{-}E_{Na})$, with $i = 1.2,3\ldots$, $g_{Na} = 110$ mS/cm^2, m_i and h_i determined as described in Section Materials and Methods and $E_{Na} = 62$ mV (Alle et al., 2009). The model provides a good description of the experimental results. The arrow in **Figure 5** highlights a slight secondary increase of I_{Na} during repolarization in the Engel and Jonas (2005) I_{Na} model attributable to an overlap of activation and inactivation. A similar result is not apparent in the experimental recordings.

The mean of the pooled results for I_K and $-I_{Na}$ from **Figures 1**, **5**, respectively, are shown in **Figure 6** scaled as described in Alle et al. (2009) along with the predictions of the I_{Na} model and I_K model 2 described above. The arrow in **Figure 6** highlights a slight overlap of I_{Na} with $I_K$during the AP, an energetically inefficient result (Alle et al., 2009).

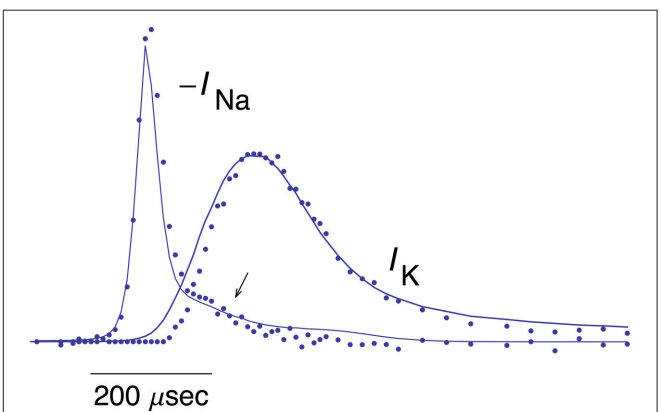

FIGURE 6 | Pooled results for $-I_{Na}$ and I_K from MFBs. The mean values of these measurements are shown here along with the theoretical curves for $-I_{Na}$ and I_K are the same as described in **Figures 1**, **5**, respectively. The arrow highlights a slight overlap in time of the two results (Alle et al., 2009).

DISCUSSION

This report provides further illustration of a method recently described for the analysis of ionic currents recorded with the AP-clamp technique (Clay, 2015). The work also provides an example of the utility of the GHK equation for the analysis of I_K from a mammalian neuronal preparation. Traditionally, those results have been described by $I_K = g_K(V\text{-}E_K)$ with g_K a constant (Hodgkin and Huxley, 1952). This expression implies, by definition, that the slope conductance for I_K at a given potential below E_K is the same as the slope conductance positive to E_K. This result is theoretically impossible when $E_K \neq 0$ because I_K is proportional to K_o^+ with V well below E_K and I_K is proportional to K_i^+ when V is well above E_K. The fully activated current-voltage relation for I_K outwardly rectifies, a result that is well described by the GHK equation (Clay, 2009). A similar result applies for I_{Na} with a caveat. The fully activated current-voltage relation for I_{Na} in squid axons in Ca^{2+}-free seawater is consistent with the GHK equation (Vandenberg and Bezanilla, 1991; their Figure 3). It inwardly rectifies since Na_o^+ is much greater than Na_i^+. Calcium ions in normal seawater partially block I_{Na} in a voltage-dependent manner with the blockade increasing as the membrane potential is hyperpolarized relative to E_{Na}. This effect counterbalances the inward rectification of I_{Na} in the absence of divalent

cations so that I_{Na} is approximately proportional to $(V\text{-}E_{Na})$ for physiological conditions over the range of potentials spanned by an AP (Vandenberg and Bezanilla, 1991). A similar mechanism may apply to I_{Na} from other preparations (Worley et al., 1986; Green et al., 1987).

One consequence of the original prediction by Hodgkin and Huxley (1952) that $I_K = g_K(V\text{-}E_K)$ is that activation curves for voltage gated K^+ channels have typically been determined by normalizing a family of I_K records using $(V\text{-}E_K)$. An activation curve with a shallow voltage dependence is obtained (open circles, **Figure 2**). In contrast, normalization of those results by GHK$[(V\text{-}E_K)]$ yields an activation curve having a steepness similar to that noted by Sigworth (2003) for voltage-gated K^+ channels. Moreover, the revised K^+ channel activation curve is similar to the Na^+ channel activation curve (**Figure 4**). High sensitivity of these channels to voltage is important because cellular voltage changes are small (Sigworth, 2003).

Models 1 and 2 for I_K both fail to account for the delay in the rising phase of this component during an AP (**Figures 1**, **6**), a result that is similar to the Cole and Moore (1960) effect in squid axons. Specifically, the delay in the rising phase of I_K following a voltage clamp step from relatively negative holding potentials is greater than the prediction of the Hodgkin and Huxley (1952) n^4 model (Cole and Moore, 1960). This result is significant in squid axons even for moderately hyperpolarized holding potentials such as −75 mV (Figure 5; Clay et al., 2008). The discrepancy between theory and experiment reported here for the rising phase of I_K elicited during AP-clamp from a holding potential of −80 mV in MFBs is a corollary of the Cole and Moore (1960) effect.

The I_K component underlying repolarization in rat hippocampal MFBs is the result of the entry of K^+ through a mixture of channels, Kv1, Kv3, and BK (Alle et al., 2011). BK channels appear not to be significant for basal APs, i.e., APs recorded under normal physiological conditions (Alle et al., 2011). The model of I_K in MFB's by Engel and Jonas (2005) is based, implicitly, on the assumption of a homogeneous population of K^+ channels. They noted that their model provided "a relatively accurate description of the voltage-dependence of activation of K^+ channels in MFBs." This view is not necessarily at odds with the results of Alle et al. (2011) especially with regard to Kv, channels that are activated rapidly. The kinetics of Kv1 and Kv3 may well be described by the same, or similar, Hodgkin and Huxley (1952) type model. In any event the falling phase of I_K obtained in AP-clamp from MFBs is consistent with a homogeneous population of K^+ channels with their fully-activated current-voltage relation described by GHK$(V\text{-}E_K)$.

The emphasis in this report is on a method, for analyzing ionic currents in neurons with an application to MFBs. The method is general. It can be applied to ionic currents in any excitable cell for which a specific blocker is available, such as TTX for I_{Na}. The method requires a digitized representation of an experimentally recorded AP as well as a model of the ionic current in question obtained from voltage clamp step results such as the Hodgkin and Huxley (1952) m^3h model for I_{Na}. The analysis given above for I_{Na} in MFBs is largely confirmatory of the m^3h model as given by Engel and Jonas (2005). The analysis for I_K in MFBs reveals two discrepancies between experiment and the Hodgkin and Huxley (1952) model of I_K, one concerning the rising phase of I_K during an AP similar to the Cole and Moore (1960) effect and a discrepancy in the falling phase that can be accounted for by changing the fully-activated current-voltage for I_K from a linear dependence upon the K^+ driving force to the GHK dependence on $(V\text{-}E_K)$. The method provides a complementary test of models constructed from voltage step results. An AP-clamp rapidly scans the range of membrane potentials corresponding to this waveform. In this way the GHK dependence of I_K on $(V\text{-}E_K)$ can be elucidated for the physiological range of membrane potentials more readily than is possible with voltage steps.

The original work of Hodgkin and Huxley (1952) continues to influence the design and analysis of experimentals in membrane neuroscience. The method described in this report provides a variation of their approach that can yield additional insight to the relationship between membrane excitability and the ionic currents that underlie excitability.

ACKNOWLEDGMENTS

This research was supported by the Intramural Research Program of the National Institute of Neurological Disorders and Stroke, National Institutes of Health, Bethesda, Maryland USA. The author gratefully acknowledges Dr. Henrik Alle for providing a table of digitized results from Alle et al. (2009).

SUPPLEMENTARY MATERIAL

The Supplementary Material for this article can be found online at: http://journal.frontiersin.org/article/10.3389/fncel.2015.00514

REFERENCES

Alle, H., Kubota, H., and Geiger, J. R. P. (2011). Sparse but highly efficient K_v3 outpace BK_{Ca} channels in action potential repolarization at hippocampal mossy fiber boutons. *J. Neurosci.* 31, 8001–8012. doi: 10.1523/JNEUROSCI.0972-11.2011

Alle, H., Roth, A., and Geiger, J. R. P. (2009). Energy-efficient action potentials in hippocampal mossy fibers. *Science* 325, 1405–1408. doi: 10.1126/science.1174331

Bean, B. P. (2007). The action potential in mammalian central neurons. *Nat. Rev. Neurosci.* 8, 451–465. doi: 10.1038/nrn2148

Bezanilla, F., and Armstrong, C. M. (1972). Negative conductance caused by the entry of sodium and cesium ions into the potassium channels of squid axons. *J. Gen. Physiol.* 60, 588–608. doi: 10.1085/jgp.60.5.588

Clay, J. R. (2009). Determining K^+ channel activation curves from K^+ channel currents often requires the Goldman-Hodgkin-Katz equation. *Front. Cell. Neurosci.* 3:20. doi: 10.3389/neuro.03.020.2009

Clay, J. R. (2015). A novel description of ionic currents recorded with the action potential clamp technique: application to excitatory currents in suprachiasmatic nucleus neurons. *J. Neurophysiol.* 114, 707–716. doi: 10.1152/jn.00846.2014

Clay, J. R., Paydarfar, D., and Forger, D. B. (2008). A simple modification of the Hodgkin and Huxley equations explains type 3 excitability in squid axons. *J. R. Soc. Interface* 5, 1421–1428. doi: 10.1098/rsif.2008.0166

Cole, K.S., and Moore, J.W. (1960). Potassium ion current in the squid giant axon: dynamic characteristic. Biophys. J. 1, 1–14.

Crotty, P., Sangrey, T., and Levy, W. B. (2006). Metabolic costs of action potential velocity. *J. Neurophysiol.* 96, 1237–1246. doi: 10.1152/jn.01204.2005

Engel, D., and Jonas, P. (2005). Presynaptic action potential amplification by voltage-gated Na^+ channels in hippocampal mossy fiber boutons. *Neuron* 45, 405–417. doi: 10.1016/j.neuron.2004.12.048

Fohlmeister, J. F. (2015). Voltage-gating by molecular subunits of Na^+ and K^+ ion channels: higher-dimensional cubic kinetics, rate constants, and temperature. *J. Neurophysiol.* 113, 3759–3777. doi: 10.1152/jn.00551.2014

French, R. J., and Wells, J. B. (1977). Sodium ions as blocking agents and charge carriers in the potassium channel of the squid giant axon. *J. Gen. Physiol.* 70, 707–724. doi: 10.1085/jgp.70.6.707

Geiger, J. R. P., and Jonas, P. (2000). Dynamic control of presynaptic Ca^{2+} inflow by fast-inactivating K^+ channels in hippocampal mossy fiber boutons. *Neuron* 28, 927–939. doi: 10.1016/S0896-6273(00)00164-1

Green, W. N., Weiss, L. B., and Anderson, O. S. (1987). Batrachotoxin-modified sodium channels in planar lipid bilayers. *J. Gen. Physiol.* 89, 841–872. doi: 10.1085/jgp.89.6.841

Hanlon, M. R., and Wallace, B. A. (2002). Structure and function of voltage-dependent ion channel regulatory beta subunits. *Biochemistry* 41, 2886–2894. doi: 10.1021/bi0119565

Hodgkin, A. L., and Huxley, A. F. (1952). A quantitative description of membrane current and its application to conduction and excitation in nerve. *J. Physiol.* 117, 500–544. doi: 10.1113/jphysiol.1952.sp004764

Jackson, A. C., Yao, G. L., and Bean, B. P. (2004). Mechanism of spontaneous firing in dorsomedial suprachiasmatic nucleus neurons. *J. Neurosci.* 24, 7985–7998. doi: 10.1523/JNEUROSCI.2146-04.2004

Jan, L. Y., and Jan, Y. N. (1997). Cloned potassium channels from eukaroytes and prokaroytes. *Annu. Rev. Neurosci.* 20, 91–123. doi: 10.1146/annurev.neuro.20.1.91

Llinás, R., Sugimori, M., and Simon, S. M. (1982). Transmission by presynaptic spike-like depolarization in the squid giant synapse. *Proc. Natl. Acad. Sci. U.S.A.* 79, 2415–2419. doi: 10.1073/pnas.79.7.2415

MacKinnon, R. (1991). Determination of the subunit stoichiometry of a voltage-activated potassium channel. *Nature* 350, 232–235. doi: 10.1038/350232a0

MacKinnon, R. (1995). Pore loops: an emerging theme in ion channel structure. *Neuron* 14, 889–892. doi: 10.1016/0896-6273(95)90327-5

Sengupta, B., Stemmler, M., Laughlin, S. B., and Niven, J. E. (2010). Action potential energy-efficiency varies among neuron types in vertebrates and invertebrates. *PLoS Comp. Biol.* 6:e1000840. doi: 10.1371/journal.pcbi.1000840

Sigworth, F. J. (2003). Life's transistors. *Nature* 423, 21–22. doi: 10.1038/423021a

Vandenberg, C. A., and Bezanilla, F. (1991). Single-channel, macroscopic, and gating currents from sodium channels in the squid giant axon. *Biopyhs. J.* 60, 1499–1510. doi: 10.1016/S0006-3495(91)82185-3

Worley, J. F., French, R. J., and Krueger, B. K. (1986). Trimethyloxonium modification of single batrachotoxin-activated sodium channels in planar bilayers. Changes in unit conductance and in block by saxitoxin and calcium. *J. Gen. Physiol.* 87, 327–349.

Conflict of Interest Statement: The author declares that the research was conducted in the absence of any commercial or financial relationships that could be construed as a potential conflict of interest.